

Mechanisms of filtration failure during postischemic injury of the human kidney. A study of the reperfused renal allograft.

V Alejandro, ... , W Deen, B D Myers

J Clin Invest. 1995;95(2):820-831. <https://doi.org/10.1172/JCI117732>.

Research Article

Postischemic filtration failure in experimental animals results primarily from depression of the transcapillary hydraulic pressure difference (ΔP), a quantity that cannot be determined in humans. To circumvent this limitation we determined the GFR and each of its remaining determinants in transplanted kidneys. Findings in 12 allografts that exhibited subsequent normofiltration (group 1) were compared with those in 11 allografts that exhibited persistent hypofiltration (group 2). Determinations were made intraoperatively in the exposed graft after 1-3 h of reperfusion. GFR (6 ± 2 vs 29 ± 5 ml/min) and renal plasma flow by Doppler flow meter (140 ± 30 vs 315 ± 49 ml/min) were significantly lower in group 2 than group 1. Morphometric analysis of glomeruli obtained by biopsy and a structural hydrodynamic model of viscous flow revealed the glomerular ultrafiltration coefficient to be similar, averaging 3.5 ± 0.6 and 3.1 ± 0.2 ml/(min·mmHg) in group 2 vs 1, respectively. Corresponding values for plasma oncotic pressure were also similar, averaging 19 ± 1 vs 21 ± 1 mmHg. We next used a mathematical model of glomerular ultrafiltration and a sensitivity analysis to calculate the prevailing range for ΔP from the foregoing measured quantities. This revealed ΔP to vary from only 20-21 mmHg in group 2 vs 34-45 mmHg in group 1 ($P < 0.001$). Further morphometric analysis [...]

Find the latest version:

<https://jci.me/117732/pdf>



Mechanisms of Filtration Failure during Postischemic Injury of the Human Kidney

A Study of the Reperfused Renal Allograft

Veludina Alejandro,* John D. Scandling, Jr.,* Richard K. Sibley,[‡] Donald Dafoe,[§] Edward Alfrey,[§] William Deen,^{||} and Bryan D. Myers*

*Division of Nephrology, [‡]Department of Pathology, and [§]Department of Surgery, Stanford University School of Medicine, Stanford, California 94305; and ^{||}Department of Chemical Engineering, Massachusetts Institute of Technology, Cambridge, Massachusetts 02139

Abstract

Postischemic filtration failure in experimental animals results primarily from depression of the transcapillary hydraulic pressure difference (ΔP), a quantity that cannot be determined in humans. To circumvent this limitation we determined the GFR and each of its remaining determinants in transplanted kidneys. Findings in 12 allografts that exhibited subsequent normofiltration (group 1) were compared with those in 11 allografts that exhibited persistent hypofiltration (group 2). Determinations were made intraoperatively in the exposed graft after 1–3 h of reperfusion. GFR (6 ± 2 vs 29 ± 5 ml/min) and renal plasma flow by Doppler flow meter (140 ± 30 vs 315 ± 49 ml/min) were significantly lower in group 2 than group 1. Morphometric analysis of glomeruli obtained by biopsy and a structural hydrodynamic model of viscous flow revealed the glomerular ultrafiltration coefficient to be similar, averaging 3.5 ± 0.6 and 3.1 ± 0.2 ml/(min · mmHg) in group 2 vs 1, respectively. Corresponding values for plasma oncotic pressure were also similar, averaging 19 ± 1 vs 21 ± 1 mmHg. We next used a mathematical model of glomerular ultrafiltration and a sensitivity analysis to calculate the prevailing range for ΔP from the foregoing measured quantities. This revealed ΔP to vary from only 20–21 mmHg in group 2 vs 34–45 mmHg in group 1 ($P < 0.001$). Further morphometric analysis revealed the diameters of Bowman's space and tubular lumens, as well as the percentage of tubular cells that were necrotic or devoid of brush border, to be similar in the two groups. We thus conclude (a) that ΔP depression is the predominant cause of hypofiltration in this form of postischemic injury; and (b) that afferent vasoconstriction rather than tubular obstruction is the proximate cause of the ΔP depression. (*J. Clin. Invest.* 1995; 95:820–831.) **Key words:** filtration dynamics • glomerular morphometry • tubular morphometry • ultrafiltration coefficient • filtration pressure

Introduction

Transplantation of a normal kidney is a widely used and effective therapy for patients with end-stage renal failure. To effect-

ate the transplantation, however, requires interruption of blood flow from the time that the kidney is procured from the donor until vascular anastomosis to the recipient is complete. To minimize renal injury during this ischemic interval, oxygen-requiring transport processes are slowed by maintaining kidney temperature as close as possible to 4°C. Nevertheless, postischemic injury to the allograft remains a common complication of the transplantation procedure (1). Like postischemic injury to the native kidney, it is characterized by a profound depression of the GFR. The latter phenomenon results in a failure of the recipient's azotemia to resolve promptly in the wake of the transplantation, and is often referred to as delayed graft function. Unrecognized acute rejection can, of course, also contribute to delayed graft function, but is seldom an important factor in the first week after transplant. Thus, as judged by a subsequent need to provide dialysis treatment in the first postoperative week, postischemic allograft injury has been estimated to occur with an incidence of 30–40%.

Our understanding of the phenomenon of postischemic filtration failure derives largely from the study of experimental animals, in which blood flow to the native kidney has been transiently interrupted for between 30 and 60 min. The profound depression of GFR which follows subsequent reperfusion of the kidney lasts for seven or more days, and has been attributed mainly to a decline in the glomerular transcapillary hydraulic pressure difference (ΔP).¹ The initial fall in this outward driving force for ultrafiltrate formation has been shown to be a consequence of obstruction of tubules by necrotic cell debris, with a resultant increase in the upstream hydraulic pressure in Bowman's space (2–5). Subsequent afferent arteriolar constriction has been found to lower glomerular capillary hydraulic pressure some 24–48 h after reperfusion, thereby depressing the ΔP further (2, 5–8).

Because hydraulic pressure cannot be determined in either the capillaries or the Bowman's space of human glomeruli, it has not been possible to confirm a GFR-lowering role for reduced ΔP in patients with postischemic renal injury. In an effort to circumvent this limitation, we have exploited the accessibility of the exposed and reperfused allograft during transplantation surgery to determine the GFR and estimate each of its remaining determinants. We then applied these quantities to a mathematical model of glomerular ultrafiltration and calculated the level of ΔP that is likely to have prevailed during the presence or absence of postischemic filtration failure.

1. *Abbreviations used in this paper:* A_G , cross-sectional areas of the glomerular tuft; ΔP , glomerular transcapillary hydraulic pressure difference; k , hydraulic permeability; K_f , glomerular ultrafiltration coefficient; PAH, para-aminohippurate; π_A , oncotic pressure; π_{GC} , glomerular capillary oncotic pressure; RPF, renal plasma flow.

Address correspondence to Bryan D. Myers, Division of Nephrology, Room S201, Stanford University Medical Center, 300 Pasteur Drive, Stanford, CA 94305-5114.

Received for publication 5 July 1994 and in revised form 19 September 1994.

J. Clin. Invest.

© The American Society for Clinical Investigation, Inc.

0021-9738/95/02/0820/12 \$2.00

Volume 95, February 1995, 820–831

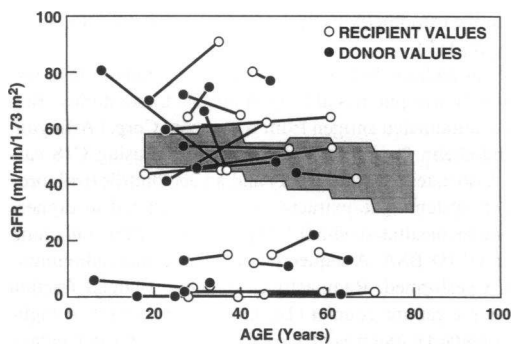


Figure 1. Relationship between GFR (iothalamate clearance) and age on the third postoperative day. The closed symbols represent values of GFR corrected for body surface area (per 1.73 m²) of the donor vs donor age. The open symbols are corresponding values for the recipients. Each donor–recipient pair is joined by a line. The shaded area represents the mean \pm 1 SD for the one-kidney GFR (inulin clearance per 1.73 m² \div 2) for each of the third through eighth decades in 104 healthy volunteers. 12 kidney transplants exhibiting normal or elevated one-kidney GFR comprise group 1 (prompt function). 11 kidney transplants exhibiting depressed GFR comprise group 2 (delayed function).

Methods

Patient population

23 consecutive patients undergoing renal transplantation at our institution gave informed consent to a study of allograft function. Each was studied according to a protocol, which had been approved previously by the Panel for Research in Human Subjects at Stanford University. They ranged in age from 18 to 71 yr, and 13 were male. The transplant was donated by a living parent or sibling in 7 instances and was obtained from a cadaveric source in the remaining 16 cases. The donors were of similar age to the recipients, spanning a range of 6 to 65 yr. The GFR, measured as the clearance of iothalamate on postoperative day 3, was used to divide the patients into two groups. Group 1 ($n = 12$) was comprised of 12 subjects who had a normal age-adjusted GFR for a single kidney (Fig. 1). Group 2 was comprised of the remaining 11 patients who exhibited marked depression of the GFR, a finding which was attributed to postischemic injury to the allograft (Fig. 1). To avoid confounding effects on GFR of cyclosporine, a vasoconstrictor substance (9, 10), initiation of treatment with this immunosuppressive agent was withheld until after completion of the iothalamate clearance on postoperative day 3.

Transplantation procedures

(a) *Management of living donors.* An extensive preoperative evaluation was undertaken to ensure that renal function and anatomy were normal in each living donor. Nephrectomy was performed under isoflurane anesthesia on the day of transplantation. After dissecting the kidney free of surrounding fat, the vascular pedicle was isolated and the renal artery and vein skeletonized. The ureter was dissected down to the level of the pelvic brim. Clamps were then placed across both vessels and the ureter, and each structure was transected. The kidney was submerged in a basin of iced lactated Ringer's solution and the renal circulation flushed with UW preservation solution until the venous effluent was clear. Thereafter, the kidney remained in cold storage in the iced Ringer's solution until the transplantation 30–60 min later.

(b) *Management of cadaveric donors.* All cadaveric donors in this series died of a severe brain injury. Crystalloid fluids and dopamine (0.1–0.5 μ g/kg per min) were infused in an effort to maintain systolic blood pressure above 90 mmHg and urine flow above 50 ml/h. The number and duration of hypotensive episodes were recorded. Cadaveric organ procurement was coordinated by the California Transplant Donor Network. A neurologist in each participating center diagnosed brain

death using clinical criteria. With the heart still beating, the donor was taken to an operating room, where the renal circulation was exposed. To minimize the warm ischemic time, the kidneys were first cooled in situ by flushing the renal circulation with cold University of Wisconsin (UW) preservation solution. The kidneys were then removed and stored in iced UW solution at 4°C until transplantation.

(c) *Management of transplant recipients.* 18 recipients in the present series were receiving maintenance hemodialysis therapy and three chronic ambulatory peritoneal dialysis. The remaining two subjects (both subsequently members of group 1) were never dialyzed, receiving their transplantation from living donors when therapy for their end-stage renal failure became urgent because of a GFR that was estimated to be well below 10 ml/min. All recipients on maintenance dialysis were dialyzed within the 24 h preceding the transplantation. Peritoneal dialysis catheters were drained and capped before surgery. Preoperative levels of creatinine, height, weight, and blood pressure were recorded in each instance.

General anesthesia was induced with narcotic agents and maintained with isoflurane. An indwelling bladder catheter and a central venous line were inserted after induction of anesthesia. The extraperitoneal space was entered through a lower quadrant abdominal incision. The external iliac artery and vein were identified, skeletonized for a distance of 8 cm, and clamped proximally and distally. Methylprednisolone 1 g and azathioprine (10 mg/kg) were then infused intravenously. The kidney graft was removed from the iced storage solution and the renal artery and vein anastomosed end-to-side to the corresponding recipient iliac vessels. All clamps were then released. The “rewarming time” (from the end of cold storage until completion of the anastomoses) was recorded. Mannitol (0.5 g/kg) was infused just before release of the vascular clamps. Each recipient's bladder was filled with an irrigating solution containing neomycin, bacitracin, and heparin. The donor ureter was then spatulated, the recipient bladder mucosa incised, and a uretero-neocystostomy created. The detrusor muscle was reapproximated over the ureteroneocystostomy to create an antireflux tunnel. Crystalloid solutions were infused throughout the operative procedure to maintain central venous pressure > 10 mmHg.

(d) *Postoperative immunosuppression.* The immunosuppressive regime for the first 10 days was comprised of antithymocyte globulin (ATGAM; The Upjohn Co., Kalamazoo, MI), prednisone, and azathioprine. The daily ATGAM dose of 20 mg/kg was adjusted downwards in the event of leukopenia or thrombocytopenia. Prednisone dosage was tapered from an initial level of 1.5 to 1.0 mg/kg per d. Azathioprine dosage was similarly tapered from 5 to 2 mg/kg per d. Cyclosporine therapy was introduced only after the third postoperative day, when allograft function was judged to be adequate because of a spontaneous fall in the serum creatinine level to below 3 mg/dl. Body weight, blood pressure, serum creatinine, and urine output were recorded daily.

Protocol

Evaluation of early allograft function. The GFR and its determinants were evaluated during the first 3 h after reperfusion of the allograft. Renal blood flow was determined 45 min after reperfusion by Doppler flow probe using an ultrasonic transit time flow meter (HT 107; Transonic Systems Inc., Ithaca, NY). A snugly fitting flow probe of 12–16 mm in diameter was placed around the renal vein. The iliac fossa was then filled with saline to optimize ultrasonic determinations. Triplicate determinations were recorded on a precalibrated digital readout at 2-min intervals. The coefficient of variation between measurements was 15%, and renal blood flow was expressed as the median value of the three determinations. Mean arterial pressure was simultaneously determined by dynamap and central venous pressure by transducer. Renal vascular resistance was calculated by dividing the arterio–venous pressure drop by renal blood flow. Renal plasma flow (RPF) was calculated from the product of renal blood flow and the fractional hematocrit of venous blood. 30-ml samples of blood were then drawn from both the renal vein and the iliac vein for determination of plasma renin activity and endothelin I levels. Samples were placed in cooled EDTA-coated

polypropylene tubes and centrifuged. The supernatant plasma was removed and stored at -70°C until the day of immunoassay.

Upon completion of the foregoing hemodynamic determinations an open surgical biopsy was taken from the cortex of the allograft. The biopsy measured ~ 6 mm in length, 4 mm in width, and 3 mm in depth. It was divided into portions for examination by light and electron microscopy. The portion for light microscopy was fixed in Zenker's fluid, dehydrated, and embedded in paraffin. The portion for electron microscopy was fixed in 2.5% glutaraldehyde buffered with cacodylate and postfixed in 2% osmium tetroxide for 60 min. The fixed tissue was then embedded in epon after passage through a series of graded ethanols.

Once the surgical procedure was complete, the irrigating solution was rinsed out of the bladder to permit determination of the GFR by the clearance technique. A 30% solution of iohalamate was given as a bolus followed by a sustaining infusion to maintain plasma iohalamate levels constant, as described by us previously (11). After a 60-min period of equilibration, arterial and venous pressures were determined and venous plasma sampled for the determination of oncotic pressure (π_A). Two timed urine collections, each of 30–60 min duration, were then made via the Foley bladder catheter. Each urine collection was bracketed by a 10-ml sample of venous blood. Plasma and urine samples were then assayed for iohalamate and true creatinine levels. Our original intention to use the iohalamate clearance as the primary measure of allograft GFR was thwarted by the presence of substances which interfered in the iohalamate assay, presumably anesthetic agents or other drugs given during the surgical procedure. We accordingly substituted the clearance of endogenous creatinine as the primary measure of GFR during this early evaluation of allograft function. Justification for this substitution was provided by the demonstration that values for the simultaneous clearances of creatinine and iohalamate were similar under the conditions of the present study (Appendix 1). We also determined the osmolality and sodium concentration of each urine and plasma sample, and used the urine-to-plasma osmolality ratio and the fractional excretion of sodium (FE_{Na}) as indices of tubular function (12, 13).

Evaluation of postoperative allograft function. A mathematical model of creatinine kinetics was used to calculate the prevailing creatinine clearance for each of the first 10 postoperative days (14). A more formal evaluation of renal function was undertaken on the morning of postoperative day 3, before the Foley bladder catheter was removed. The clearances of iohalamate, para-aminohippurate (PAH) and creatinine during four consecutive 30-min urine collections were determined. Interfering substances were no longer present in recipient serum at this time, and the clearance of iohalamate was used as the primary measure of GFR. Other determinations performed during the day 3 clearance study included arterial and central venous pressures, π_A , circulating levels of endothelin I and plasma renin activity, and the aforementioned indices of tubular function.

Laboratory determinations. A high pressure liquid chromatography system with an online ultraviolet light detector was used to assay iohalamate and PAH at 263 nm (No. 6A; Instrumentation Shimadzu, Kyoto, Japan). Ultrafiltrates of plasma and diluted urine were injected onto a reverse-phase column (No. C18, 5 μm , Ultrasphere; Beckman Instruments, San Ramon, CA). The mobile phase was 3.5% acetonitrile in 10 mM triethylamine at pH = 3.0 and a flow rate of 1.0 ml/min. Iohalamate and PAH concentration was determined from the peak area of each solute, corresponding to column retention times of 14 and 10 min, respectively (11). The concentration of creatinine in urine and plasma was determined by an automated, rate-dependent picrate method using a creatinine analyzer (analyzer II; Beckman Instruments). This method minimizes the influence of slow-reacting noncreatinine chromogens and thus provides an estimate of true creatinine concentration. Osmolality of urine and plasma was measured by freezing point depression, using an osmometer (model CDII; Advanced Instruments, Inc., Needham Heights, MA), while corresponding concentrations of sodium were determined by flame photometry (Instrumentation Laboratories, Lexington, MA). The oncotic pressure in venous plasma was taken to be the same as that entering the glomerular tuft (π_A), and was measured

directly by membrane osmometry using a colloid osmometer (No. 4400; Wescor Inc., Logan, UT).

Plasma levels of endothelin I were determined by radioimmunoassay. Specific antibody was purchased from Peninsula Laboratories (Belmont, CA) and radioiodinated antigen from Amersham Corp. (Arlington Heights, IL). Endothelin I was extracted from plasma using C18 cartridges (Waters Associates, Milford, MA) and an acetonitrile/trifluoroacetic acid elution system. The extracts were concentrated to dryness by evaporation and reconstituted with 0.1 M phosphate buffer containing 1% Triton-100 and 0.1% BSA. A sequential nonequilibrium radioimmunoassay was then performed. Radioactivity of the ^{125}I -bound fraction was measured using a gamma counter (Beckman Instruments). A logit-log transformed standard curve was then used to calculate the percentage of endothelin I bound. Plasma renin activity was determined from the rate of angiotensin I generated at pH = 6.0 using a radioimmunoassay kit provided by Clinical Assays Inc. (Stillwater, MN).

Morphological studies

(a) Glomerular morphometry. 1- μm thick sections of the paraffin-embedded biopsy material were cut and stained with periodic acid Schiff reagent. A dedicated computer system (Southern Micro Instruments, Atlanta, GA) consisting of a video camera, monitor, light microscope, and digitizing tablet was used to perform measurements (15, 16). The average number of glomeruli examined per biopsy was 25 in group 1 and 32 in group 2. The outline of each Bowman's capsule and glomerular tuft in the cross-section was traced onto the digitizing tablet at a magnification of 900. The cross-sectional areas within Bowman's capsule (A_{BC}) and of the glomerular tuft (A_{G}) were computed using area perimeter analysis. The difference between A_{BC} and A_{G} yielded the area of Bowman's space (A_{BS}). Glomerular volume (V_{G}) was calculated from A_{G} and corrected to account for the tissue shrinkage associated with paraffin embedding, using a linear shrinkage factor (f_s) (17).

$$V_{\text{G}} = \frac{\beta}{d} A_{\text{G}}^{3/2} f_s^{-3} \quad (1)$$

where β is a dimensionless shape coefficient ($\beta = 1.38$ for spheres) and d is a "size distribution coefficient" which is introduced to account for variations in glomerular size. We used $d = 1.1$, which corresponds to a distribution of glomerular sizes with a standard deviation of 25% of the mean size (17). We have determined that, in our experimental procedure for tissue fixation, the value of the shrinkage factor is $f_s = 0.86$.

Toluidine blue-stained 1- μm sections of the epon-embedded material were examined to select the two glomeruli closest to the center of the block. Ultrathin sections (60–70 nm) of these glomeruli were next cut, stained with uranyl acetate and lead citrate, and photographed. A complete montage of each glomerulus was prepared at a magnification of 2,820. Point and intercept counting was then used to determine the peripheral capillary surface area (S), which was defined as the interface between the peripheral capillary wall and epithelium, and calculated as

$$S = s_v V_{\text{G}} \quad (2)$$

where S_v is the surface density of peripheral capillary wall (expressed as length of peripheral capillary wall per unit cross-sectional area of glomerulus). Eight electron photomicrographs ($\times 11,280$) were then obtained from each of the two glomerular profiles to evaluate the thickness of the glomerular basement membrane and frequency of epithelial filtration slits (18). The harmonic mean basement membrane thickness (δ_{bm}) was calculated for each individual from the measured (apparent) harmonic mean thickness (δ_{bm}') by

$$\delta_{\text{bm}} = \frac{8}{3\pi} \delta_{\text{bm}}' \quad (3)$$

where $8/(3\pi)$ is a correction factor derived by Jensen et al. (19) to account for the random angle of sectioning. The filtration slit frequency (FSF) was determined by counting the total number of slits captured on the electron photomicrographs and dividing this number by the corre-

sponding length of the peripheral capillary wall. The mean distance between filtration slits (W) was computed as

$$W = \frac{2}{\pi} \frac{1}{FSF} \quad (4)$$

where $2/\pi$ is a correction factor derived by Drumond et al. (18) to account for the random angle of sectioning.

(b) *Tubular morphometry.* Abnormalities of tubulo-interstitial structure were first assessed by light microscopy using 1- μm sections stained with periodic acid Schiff reagent. An 11×11 square grid was inserted into the eye piece of the microscope. Point and intercept counting of seven grid fields at a magnification of 900 was used to calculate the cross-sectional area of all tubules in the seven fields, and separately, of the tubular lumina. Point counting at $\times 60$ was also used to calculate the fraction of cortex occupied by interstitium in each field, where interstitial area is defined as that outside of tubular and vascular structures other than peritubular capillaries (16). The percentage of proximal tubular cells which had undergone necrosis was also estimated. Point counting was used to estimate the number of cells with pyknotic nuclei in each field, whether such cells were in their normal location or had sloughed off the tubular basement membrane and entered the tubular lumen. The loss of tubular brush border was evaluated by electron microscopy. Undamaged proximal tubules far from the edge of the biopsy were identified in toluidine blue-stained sections of 1 μm thickness. Ultrathin sections (60–70 nm) of the selected tubules were placed on slotted copper grids and photographed at a final magnification of 5,640. The brush border associated with the apical membrane of each tubular cell was evaluated and classified as normal, diminished, or entirely absent.

Calculations

(a) *Glomerular capillary oncotic pressure (π_{GC}).* We computed π_{GC} from the arithmetic mean of π_A and π_E , which are the respective oncotic pressures of plasma entering the afferent and efferent arterioles. The π_A was assumed to be the same as that measured directly in systemic venous blood. The π_E was calculated as follows

$$\pi_E = \frac{\pi_A}{1 - FF} \quad (5)$$

where FF is the filtration fraction. That π_{GC} can be equated with the arithmetic mean of π_A and π_E assumes a linear rise in oncotic pressure as plasma flows axially along the glomerular capillaries, an assumption which we have shown to be accurate to within 0.5 mmHg (20).

(b) *Glomerular ultrafiltration coefficient (K_f).* The overall K_f for the transplanted kidney is the product of the glomerular capillary hydraulic permeability (k) and the total surface area available for filtration in all glomeruli. The total surface area was computed from the single nephron value (S, determined as described above) and estimates of the total number of nephrons. The baseline value of the total number of nephrons was taken to be 1×10^6 (21). The effective hydraulic permeability was estimated from the individually measured values of δ_{bm} and mean distance between filtration slits by using the structural-hydrodynamic model of Drumond and Deen (22). Briefly, that model approximates the glomerular capillary wall as consisting of a large number of repeating structural units, each unit being based on a single filtration slit. Within a structural unit are representations of the individual layers of the capillary wall, namely, the fenestrated endothelium, the basement membrane, and the epithelial filtration slits with slit diaphragms. By solving the differential equations describing viscous flow through each of these layers, and using the concept of resistances in series, a value for k is obtained. In addition to the values of δ_{bm} and W measured in the present study, a number of other quantities are needed as inputs for the calculation of k. The other quantities, which include the intrinsic (Darcy) permeability of the glomerular basement membrane and the dimensions of various other structures, were estimated from data reported for normal rats, as described in detail previously (22, 23). The values of the other

Table I. Clinical Findings

	Group 1	Group 2
Number of patients	12	11
Age (yr)	44 \pm 4	44 \pm 4
Male/Female	7/5	6/5
Living-related/Cadaveric donors	6/6	1/10
Donor mean arterial pressure (mmHg)	92 \pm 4	80 \pm 6
Cold ischemic time (h)	10 \pm 4	20 \pm 3*
Anastomosis/rewarming time (min)	33 \pm 2	40 \pm 3

* $P < 0.05$.

inputs used here are identical to those given in Table 1 of Drumond et al. (18).

(c) *Glomerular transcapillary hydraulic pressure difference (ΔP).* The ΔP was computed from GFR, RPF, π_A , and K_f using a slightly modified version of the glomerular filtration model of Deen et al. (24). In that model the glomerular capillary network is idealized as a number of identical capillaries in parallel, and steady state mass balance equations are used to compute variations in plasma flow rate and protein concentration with distance along a representative capillary. It was assumed that ΔP is constant along a capillary. The calculations of ΔP was based on an iterative solution of the integral equation

$$\int_1^{C_E/C_A} \frac{dC}{C^2(B - A_1C - A_2C^2)} = F \quad (6)$$

to determine B, defined as $B = \Delta P/\pi_A$. The dimensionless constants in equation 6 are $F = K_f \pi_A / RPF$, $A_1 = a_1 C_A / \pi_A$, and $A_2 = 1 - A_1$; C_A and C_E are the afferent and efferent protein concentrations, respectively, and C is local protein concentration divided by C_A . The afferent protein concentration was calculated from π_A using

$$C_A = \frac{-a_1 + \sqrt{a_1^2 + 4a_2\pi_A}}{2a_2} \quad (7)$$

where the osmotic pressure coefficients are given by $a_1 = 1.629$ mmHg/(g/dl) and $a_2 = 0.2935$ mmHg/(g/dl)². The protein concentration ratio was related to the filtration fraction by $C_E/C_A = 1/(1 - FF)$, where $FF = GFR/RPF$.

The calculation of ΔP from equation 6 began by making an initial guess for B. For filtration fractions no larger than normal levels for humans (i.e., $FF \leq 0.2$), an excellent initial guess is given by

$$B \approx 1 + \frac{[1 + A_2][FF/(1 - FF)]}{1 - e^{-(1+A_2)F}} \quad (8)$$

Equation 8 was derived from a perturbation solution to the differential equation for C, and becomes exact in the limit $FF \rightarrow 0$. Starting with the initial guess for B, equation 6 was solved iteratively using a Levenberg-Marquardt algorithm, with the integral evaluated using the Romberg method, as implemented in Mathcad (Mathsoft, Cambridge, MA).

Statistical analysis

The significance of differences between the two groups was evaluated by a two-tailed, Student's *t* test or the Mann Whitney U test, depending on the distribution of the findings. All results are expressed as the mean \pm standard error.

Results

Clinical findings

The distribution of age and gender was similar in the two groups (Table I). Reflecting a higher proportion of cadaveric graft

Table II. Early Hemodynamic Findings (1 h after Reperfusion)

	Group 1	Group 2
Mean arterial pressure (mmHg)	83±2	79±1
Central venous pressure (mmHg)	17±1	16±5
Renal blood flow (ml/min)	410±52	214±50*
Renovascular resistance ([mmHg·min] per liter)	180±20	500±150*
Plasma renin activity [‡]	6.7±1.4	8.8±3.0
Endothelin I [§] (pg/ml)	8.7±0.8	9.7±0.9

* $P < 0.05$. [‡] Normal range for NaCl loading in supine position < 1.1 ng/ml per h. [§] Normal range 1.8–3.3 pg/ml.

donors in group 2 (10/11) than group 1 (6/12), the former allografts were subject to more ischemia. This was most clearly evidenced by the period of cold storage time, which was twofold longer in group 2 than group 1, 20 ± 3 vs 10 ± 4 h, respectively ($P < 0.01$). Warm ischemia, albeit partial, also tended to be greater in group 2 than in group 1. Thus, eight cadaveric donors in group 2 vs 4 in group 1 exhibited episodes of hypotension (systolic blood pressure < 90 mmHg) lasting between 10 and 240 min. This resulted in a lower value for mean arterial pressure at the time of donor nephrectomy, 80 ± 6 in group 2 vs 92 ± 4 mmHg in group 1. Similarly, rewarming ischemic time during vascular anastomosis was longer in group 2 than in group 1, 40 ± 3 vs 33 ± 2 min, respectively. However, neither of the latter two differences reached statistical significance (Table I).

Early allograft function (1–3 h)

Hemodynamic findings. Intraoperative arterial and venous pressures in the wake of allograft reperfusion were similar in the two groups (Table II). However, renal blood flow was depressed by half in the members of group 2 who went on to exhibit delayed graft function, averaging 214 ± 50 vs 410 ± 52 ml/min in group 1 with subsequent prompt function ($P < 0.05$). Renovascular resistance also differed significantly between the two groups, with the value in group 2 exceeding that of group 1 by almost threefold (Table II). Neither plasma renin activity nor plasma endothelin I levels differed between the two groups. However, the levels of each vasoconstrictor peptide were markedly elevated above the normal range (Table II). A comparison between systemic (iliac) and renal venous levels of each peptide reveals

Table III. Glomerular Function and Structure (1–3 h after Reperfusion)

	Group 1	Group 2
Glomerular filtration rate (ml/min per 1.73 m^2)	29±5	6±2*
Renal plasma flow (ml/min per 1.73 m^2)	315±49	140±30*
Filtration fraction	0.10±0.02	0.02±0.01*
Afferent oncotic pressure (mmHg)	20.8±0.9	18.5±0.9
Glomerular volume ($10^6 \mu\text{m}^3$)	1.05±0.11	1.58±0.27
Surface area/glomerulus ($10^3 \mu\text{m}^2$)	1.42±0.13	1.96±0.30
Filtration slit frequency (1/mm)	1352±39	1154±48*
Basement membrane thickness (nm)	414±17	469±24
Hydraulic permeability (k) (10^{-9} m/s per pa)	2.77±0.06	2.39±0.10*
Ultrafiltration coefficient, k_f (ml/[min × mmHg])	3.12±0.29	3.52±0.57

* $P < 0.01$.

renal secretion of renin and, in all but three cases, renal extraction of endothelin I (Fig. 2).

Glomerular function and structure. The GFR was depressed to only 6 ± 2 ml/min/ 1.73 m^2 in group 2 vs 29 ± 5 ml/min/ 1.73 m^2 in group 1 ($P < 0.01$). The RPF was also significantly lower in group 2 than in group 1 (Table III). However, depression of RPF was proportionately less than that of GFR, with the result that the filtration fraction in group 2 was profoundly depressed to only 0.02 ± 0.01 vs 0.10 ± 0.02 in group 1 ($P < 0.001$). The π_A was numerically lower by 2 mmHg in group 2 than group 1 (Table III). Consequent upon the extreme depression of the filtration fraction in group 2, there was little axial rise in oncotic pressure along the glomerular capillaries. Thus, calculated π_{GC} , the pressure that opposes the formation of filtrate, was significantly lower in group 2 than group 1, 18.8 ± 1.0 vs 22.0 ± 1.1 mmHg, respectively ($P < 0.05$, Fig. 3). By exclusion, a fall in either K_f or ΔP , or some combination of the two, must be invoked to explain the hypofiltration in group 2.

Neither glomerular volume nor S differed between the groups (Table III). The same was true for basement membrane thickness (Table III). However, there was a patchy broadening of epithelial foot processes in group 2, not seen in group 1 (Fig. 4). This resulted in a significant reduction in the frequency of epithelial filtration slits in the former, $1,154 \pm 48$ vs $1,352 \pm 39$ slits per mm, respectively ($P < 0.01$, Table III). As a result calculated k was significantly lower in the glomerular capillary walls of group 2 than in those of group 1, 2.39 ± 0.10 vs $2.77 \pm 0.06 \times 10^{-9}$ m/s per Pa, respectively ($P < 0.01$, Table

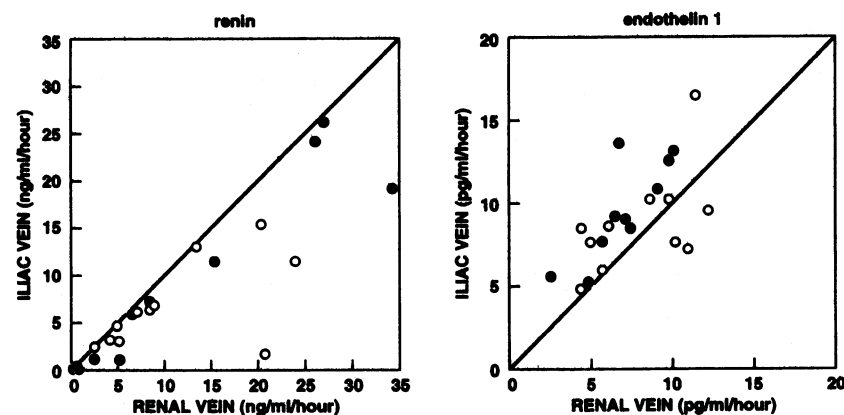


Figure 2. Plasma renin activity (left) and plasma endothelin I concentration (right) in systemic (iliac) venous blood is plotted as a function of corresponding levels in renal allograft venous blood. Group 1 subjects are depicted by open symbols and group 2 subjects by closed symbols. The line of identity is shown.

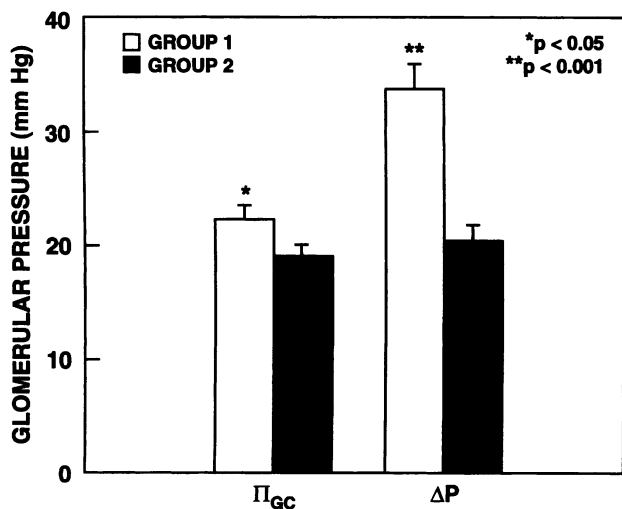


Figure 3. Calculated glomerular oncotic pressure (π_{GC} , left) and ΔP (right) 1–3 h after reperfusion. Group 1 is depicted by open bars and group 2 by closed bars. The calculations for ΔP assume 1×10^6 glomeruli per allograft, and the presence in group 2 but not in group 1 of transtubular backleak of 33% of filtrate (see Table IV). * $P < 0.05$, ** $P < 0.01$ group 1 vs group 2.

III). Of interest, the 14% reduction in k in group 2 was completely offset by a trend towards a larger value for S than in group 1 (Table III). Thus, estimated allograft K_f was not significantly different between the two groups, tending to be, if anything, slightly higher in group 2 than group 1, 3.52 ± 0.57 vs 3.12 ± 0.29 ml/(min · mmHg), respectively.

The ultrafiltration model used in the present study revealed that GFR depression in group 2 was predominantly, if not uniquely, due to ΔP depression. In performing these calculations we undertook a sensitivity analysis so as to take possible variations introduced by our assumption of total glomerular number and potential backleak of glomerular filtrate into account. Depending upon whether glomerular number per allograft was 0.7 or 1.0×10^6 , and whether or not there was backleak of filtrate, the computed ΔP in group 1 varied between 33.8 and 44.6 mmHg (Table IV). The corresponding computations for ΔP in group 2 varied between only 20.2 and 21.4 mmHg, with the value under each set of conditions significantly lower than the corresponding value in group 1 (Table IV). The hypothetical values for ΔP that minimize the disparity between the two groups are illustrated in Fig. 3. These illustrated values assume 1×10^6 glomeruli per allograft and a 33% backleak in group 2 but not group 1 (Table IV). As shown, ΔP under these “best case” conditions of comparison is 33.8 ± 2.3 mmHg in group 1, a value which exceeds corresponding π_{GC} by 12 mmHg. In contrast, the ΔP computed for group 2 is only slightly higher than the corresponding value for π_{GC} , 20.7 ± 1.4 vs 18.8 ± 1.0 mmHg, respectively (Fig. 3). Thus, our computations for ΔP suggest that postischemic filtration failure in group 2 was associated with dissipation of the net pressure for ultrafiltration.

Tubular function and structure. The allografts of both groups exhibited marked tubular dysfunction typical of postischemic tubular injury. The fractional excretion of sodium was elevated to $> 20\%$ and isostenuria was present in each group (Table V). Tubular morphometry revealed structural injury to be most prevalent in proximal tubules, and to be also similar

Table IV. Sensitivity Analysis for ΔP (mmHg)

Condition*	Group 1	Group 2
1.0×10^6 glomeruli	33.8 ± 2.3	$20.2 \pm 1.3^\ddagger$
0.7×10^6 glomeruli	3.85 ± 3.1	$20.6 \pm 1.4^\ddagger$
1.0×10^6 glomeruli/1.3 GFR	38.4 ± 3.0	$20.7 \pm 1.4^\ddagger$
0.7×10^6 glomeruli/1.3 GFR	44.6 ± 4.0	$21.4 \pm 1.7^\ddagger$

* The computations are made assuming 1.0 or 0.7×10^6 glomeruli per allograft and no backleak (lines 1 and 2) or with backleak of 33% of filtrate formed (lines 3 and 4). $^\ddagger P < 0.001$.

in the two groups (Table V). Only $\sim 2\%$ of proximal tubular cells exhibited necrosis. However, by electron microscopy, proximal tubular injury was widespread, as judged by approximately one-half of all such cells exhibiting either a marked reduction or complete absence of apical brush border (Table V, Fig. 5). Many of the necrotic tubular cells remained attached to the tubular basement membrane. As a result, only a small fraction of tubular cells, 1.1 ± 0.09 vs $1.0 \pm 0.01\%$ in group 1 and group 2, respectively, were found to have sloughed into the tubular lumen. Neither the fractional luminal area of tubules nor the fractional Bowman’s space area were significantly larger in group 2 than in group 1. Similarly, the fractional interstitial area was not different in the two groups (Table V). Thus, judged by these morphological criteria, neither tubular obstruction nor transtubular backleak of filtrate were more prominent in group 2 than in group 1.

Postoperative allograft function. A model of creatinine kinetics was used to calculate the creatinine clearance profile in each recipient from daily changes in serum creatinine levels and in body water, where the latter change was derived from daily body weight (14). As illustrated in Fig. 6, group 1 patients exhibited a progressive rise in creatinine clearance during the first four postoperative days. The mean clearance entered the normal range on postoperative day 2 and achieved a plateau of ~ 60 ml/min per 1.73 m² from day 4 onwards. Group 2, by contrast, exhibited a marked and relatively constant depression of computed creatinine clearance throughout the first postoperative week. An ensuing azotemia required one or more postoperative dialyses in 7 of the 11 members of group 2.

A more detailed evaluation of postoperative allograft function was undertaken on day 3. By this time, fluid retention was twice as marked in group 2 as in group 1 (Table VI). This was accompanied by significantly greater central venous hypertension (Table VI). Plasma renin activity in group 1 returned to the normal range. Despite the increasing hypervolemia in group 2, however, plasma renin activity remained markedly elevated, exceeding corresponding group 1 levels by more than threefold (Table VI). A similar disparity was observed for endothelin I, which on day 3 averaged 12.5 ± 3.4 in group 2 vs 5.0 ± 0.6 pg/ml in group 1 ($P < 0.05$).

Whereas GFR doubled between the operation day and postoperative day 3 in group 1 (29 ± 5 – 59 ± 4 ml/min, $P < 0.01$), this quantity remained unchanged at only 6 ± 2 ml/min in group 2. The increase in GFR in group 1 could not be attributed to changes in either RPF or π_A . Assuming that renal PAH extraction was likely normal in group 1 by postoperative day 3 (25), we have used the PAH clearance to estimate that the filtration fraction increased by 70% between the two examinations (Table



Table V. Tubular Function and Structure

	Group 1	Group 2
Urine flow rate (ml/min)	8.59±1.51	2.15±1.07*
FeNa (%)	23.2±2.0	29.2±7.1
Urine/plasma osmolality	0.98±0.02	1.00±0.03
Percent necrotic tubular cells	1.8±0.3	2.2±0.5
Percent cells with decreased brush border	43.8±3.9	52.0±4.0
Percent cells with absent brush border	6.8±1.4	6.3±1.7
Fractional luminal area	0.81±0.01	0.80±0.01
Fractional Bowman's space area	0.31±0.05	0.33±0.05
Fractional interstitial area	0.19±0.01	0.20±0.01

* $P < 0.01$.

VI). Assuming further that the essentially normal glomerular morphometry observed in this group on day 0 remained unaltered, we used K_f calculated from the intraoperative biopsy along with day 3 values for GFR, RPF, and π_A to compute the prevailing ΔP . These computations suggest that ΔP increased between the two examinations by 11 or 16 mmHg to 45.4±2.8 or 54.7±3.9 mmHg, respectively, depending upon whether the allograft contained 1.0 or 0.7 × 10⁶ glomeruli. In each hypothetical example, the increment in ΔP between the two examinations is highly significant (Fig. 7). Given constancy of π_{GC} between the two examinations (Fig. 7) and the assumption of unchanging K_f , the early doubling of GFR in group 1 appears, therefore, to be an exclusive consequence of a ΔP -mediated increase in ultrafiltration pressure.

The enhancement of GFR on postoperative day 3 in group 1 was associated with recovery of tubular function. Urinary concentrating ability was restored and FE_{NA} declined to 3.2±0.8%, a value appropriate to the 6% excess of body water and high central venous pressure observed at this time (Table VI). In contrast, sustained hypofiltration in group 2 was accompanied by persistent isosthenuria and excretion of a high fraction of the filtered sodium load (Table VI). Given this evidence of persistent tubular dysfunction, we infer that PAH extraction is likely to have been markedly impaired on postoperative day 3 (6, 26, 27). Accordingly, we have not attempted to use the PAH clearance to make estimates of values for the filtration fraction, π_{GC} , or ΔP in group 2 at this time.

Discussion

Despite storage of the donor kidney at 4°C before transplantation, we have shown postischemic injury to the human renal allograft to be invariable. Provided that the ischemic interval was brief, as was usually the case when the graft was taken from a living relative, such injury lasted for < 36 h. It was characterized by extensive reduction in apical brush border and patchy necrosis of tubular cells, notably those of the proximal tubule (28, 29). It was associated with transient impairment of sodium reabsorption, urinary concentrating ability, and glomerular ultrafiltration. When the ischemic interval was of longer

Table VI. Allograft Function on Postoperative Day 3

	Group 1	Group 2
Percent weight gain from day 0	5.5±1.7	12.0±2.1*
Mean arterial pressure (mmHg)	101±3	104±3
Central venous pressure (mmHg)	16±1	21±1 [‡]
Plasma renin activity (ng/ml per h)	1.0±0.3	3.6±1.5*
Endothelin 1 (pg/ml)	5.0±0.6	12.5±3.4*
GFR (ml/min per 1.73 m ²)	59±4	6±2 [§]
PAH clearance (ml/min per 1.73 m ²)	328±20	50±15 [§]
Filtration fraction	0.17±0.01	—
π_A (mmHg)	20.3±1.0	18.9±1.0
Urine flow rate (ml/min)	3.44±0.94	1.80±0.71
FeNa (%)	3.2±0.8	12.8±3.9 [‡]
Urine/plasma osmolality	1.46±0.10	0.95±0.05 [§]

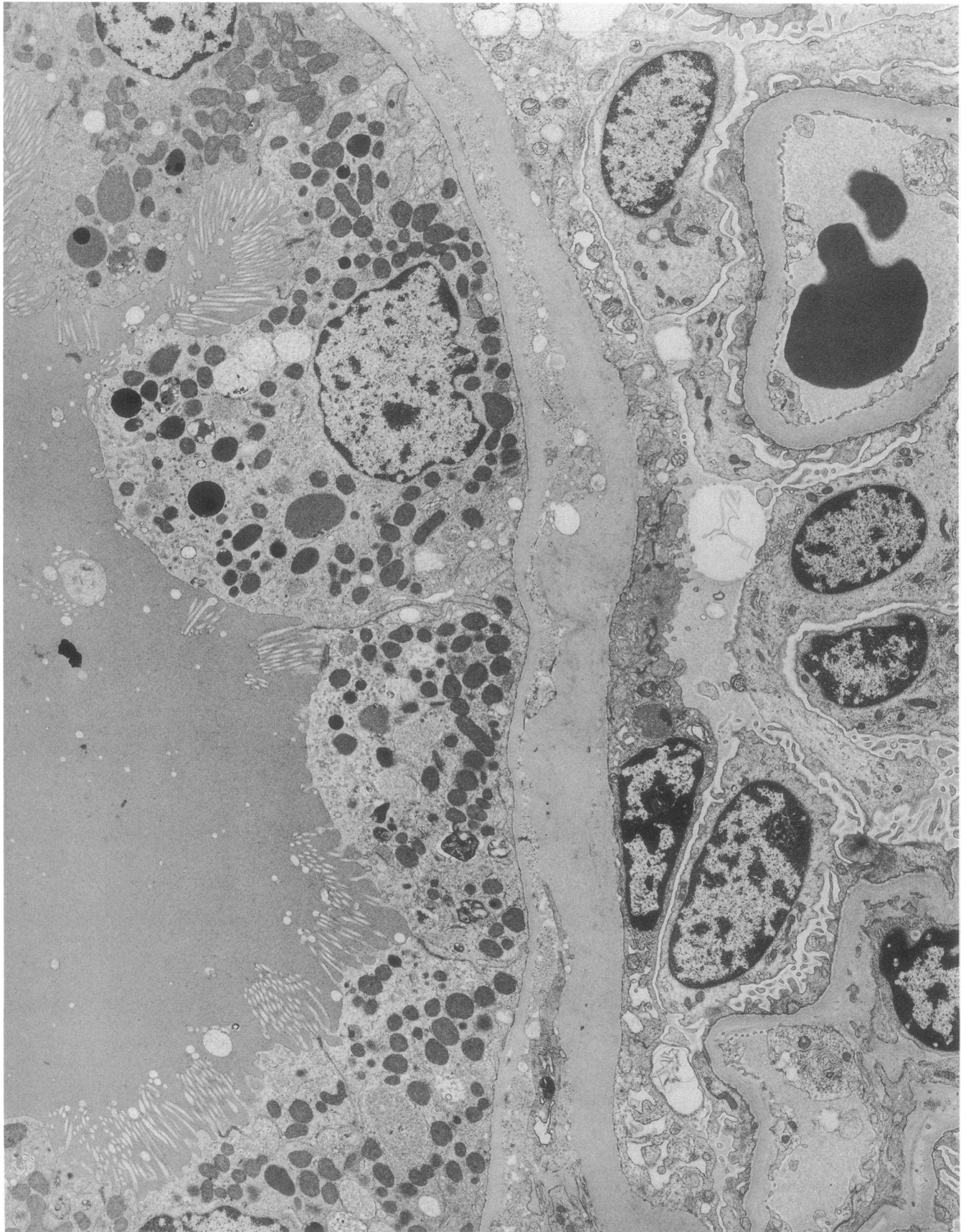
* $P < 0.05$. [‡] $P < 0.01$. [§] $P < 0.001$.

duration, as was the case in many recipients of cadaveric grafts, a more prolonged injury was manifest. In addition to persistent tubular dysfunction, it was characterized by profound hypofiltration, which lasted for > 36 h. The extent of initial microvascular injury in the immediate wake of graft reperfusion distinguished between those destined to develop a transient or sustained postischemic injury to the allograft. In contrast, the extent of the corresponding, initial injury to the tubule was not predictive of the subsequent course of allograft function.

We have attempted to elucidate the mechanism of postischemic hypofiltration by comparing each determinant of the GFR between those with a sustained injury (group 2) and those with a transient injury (group 1). Paradoxically, we found π_{GC} to be lower in the former, a finding which should have enhanced and not depressed the GFR (24). Using a morphological approach, we were also unable to demonstrate a role for depression of K_f in the genesis of hypofiltration. We did, however, observe a broadening of glomerular epithelial foot processes in those with severe hypofiltration. This finding has also been reported in animal models of postischemic acute renal failure (7, 30), and has led to K_f depression in this setting (7). In the members of group 2 in the present study, an ensuing reduction by 14% in the value for k was offset by a trend towards enhanced S . Given the limited sample of glomeruli that we were able to examine, we cannot exclude the possibility that the latter finding was spurious. Nevertheless, the focal and modest nature of the reduction in filtration slit frequency makes it unlikely that k could have been sufficiently depressed to account for the severe hypofiltration observed in the subjects of group 2 (22).

We are thus led to the conclusion that the early depression of allograft GFR in group 2 subjects was predominantly a consequence of a profound reduction in ΔP . In computing the range into which ΔP was depressed, we have attempted to account for potential errors introduced by two quantities which could not be determined, and had to be assumed. One of these is the mean number of glomeruli per human kidney, which is used to calculate K_f . This quantity has been estimated at -1×10^6 by

Figure 4. Focal foot process broadening and effacement in a representative electronphotomicrograph (×11,280) from a group 2 patient.



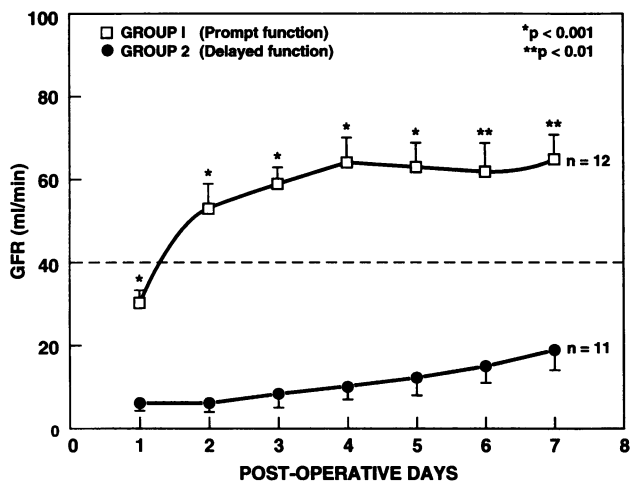


Figure 6. Mean GFR profiles of group 1 (open squares) and group 2 (closed circles) have been calculated for the first postoperative week from a model of creatinine kinetics. The dashed horizontal line indicates the bottom of the range for one-kidney GFR (40 ml/min) in 104 healthy volunteers.

one group of workers and at -0.7×10^6 by another (21, 31). Another unknown is whether or not tubular injury in the present study was accompanied by transtubular backleak of filtrate into the interstitium (13, 32, 33). The latter phenomenon would result in an underestimation by the urinary clearance technique of GFR, an input value in the mathematical model used to calculate ΔP .

Provided that the number of glomeruli was similar in each group of subjects, and regardless of the presence or absence of backleak, our computations suggest that ΔP was substantially lower in group 2 than in group 1 subjects of the present study. Table IV shows that computed ΔP in group 1 varied between 34 and 45 mmHg, a range that is similar to that estimated in the normal rat or dog by micropuncture (5, 7, 34). That these computations are reasonable is suggested further by the finding that the large increment in GFR observed over the first three days in group 1 subjects can only be satisfactorily explained by an increase in ΔP . This, too, is similar to the response after contralateral nephrectomy demonstrated by micropuncture in experimental animals (34). In contrast to values > 34 mmHg computed for ΔP in group 1, the corresponding values for ΔP in group 2 varied between only 20 and 21 mmHg, depending on the number of glomeruli used to calculate K_f and the assumption of the presence or absence of backleak of filtrate. This computed range is only 1–2 mmHg higher than the corresponding value of 19 ± 1.0 mmHg for π_{GC} (Fig. 3). Thus, as in the experimental models of postischemic acute renal failure in the rat or dog, allograft filtration failure in the present study appears to be attributable mainly to a dissipation of the net pressure for ultrafiltration (2, 3, 5).

As stated previously, the depression of ΔP that has been observed within the first few hours in experimental postischemic acute renal failure has been associated with a high hydraulic

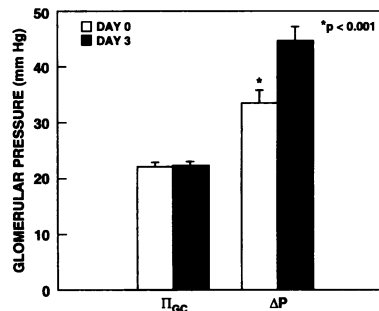


Figure 7. Serial values calculated for π_{GC} (left) and ΔP (right) in group 1 subjects. Values 1–3 h after reperfusion (open bars) are compared with those on the third postoperative day (hatched bars). * $P < 0.001$ between the two examinations.

pressure in Bowman's space due to obstruction of the pars recta of proximal tubules (4). Because our biopsy sample was too superficial to incorporate the pars recta, we are unable to exclude a similar phenomenon in the allografts of group 2 subjects in the present study. Pars recta obstruction in the postischemic rat kidney, however, was accompanied by dilatation of the upstream convolutions of the proximal tubule (4). In our assessment of tubular morphology of group 2 allografts by contrast, we were unable to find evidence of dilatation of either tubular lumina or Bowman's space (Table V). Furthermore, in keeping with the observations of Olsen and Solez and their co-workers, we observed a paucity of necrotic cells or other debris in the lumina of the tubules of the allograft (35). Conceivably, cold ischemia at 4°C ameliorated the extent of tubule cell karyorrhexis when compared to that which follows warm ischemia (36). Thus, our morphometric analysis of allograft tubular damage points away from an important contribution to the postischemic injury by tubular obstruction. This, in turn, points to afferent arteriolar constriction with an attendant fall in glomerular perfusion pressure as the primary mechanism by which glomerular filtration is brought to a halt in the freshly transplanted, human allograft. We wish to emphasize, however, that tubular necrosis has been shown to be more extensive in postischemic injury of the native than the transplanted kidney (37). We, thus, recommend that the present findings not be extrapolated to infer that tubular obstruction is not an important cause of postischemic filtration failure in the native kidney.

The high fraction of filtered sodium reaching final urine suggests that a large load of filtered sodium could have reached the macula densa, thereby mediating afferent vasoconstriction via tubulo-glomerular feedback (38). We have recently reported a loss of polarity of proximal tubular cells in the allografts of group 2 subjects, a phenomenon which could lead to impaired proximal reabsorption of sodium (39). Among other potential mediators of afferent vasoconstriction in the setting of postischemic filtration failure is the demonstrated excess of circulating levels of renin and endothelin I (40–43). Although each peptide was similarly elevated in the two groups intraoperatively, the elevation was sustained on day 3 only in the subjects of group 2. This raises the possibility that both endothelin I and angiotensin II contributed via afferent constriction to the sustained depression of ΔP that appears to underlie the persistent hypofiltration exhibited by group 2 allografts.

Figure 5. Electronphotomicrograph of proximal tubular cells in a representative group 2 patient. Note complete loss or reduction of brush border on apical membrane of several cells in the field ($\times 5,640$).

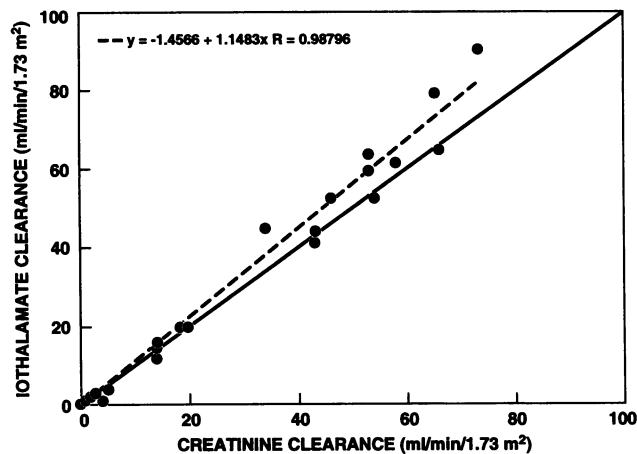


Figure 8. Iothalamate clearance is plotted as a function of simultaneous creatinine clearance on day 3, when there was no interference in the iothalamate assay. The identity (solid) and regression lines (dashed) are shown.

Persistent hyperreninemia in group 2 subjects, and the demonstration that their allografts were likely the source of the excess renin (Fig. 2), also provides indirect evidence in support of an important role for afferent vasoconstriction in the posts ischemic hypofiltration. Given that our group 2 subjects were examined in the supine position under conditions of increasing hypovolemia, and that the transplanted kidney is denervated (45), renin production should have been depressed and not stimulated (46). The only remaining stimulus for renin release that we can identify is that which is mediated by preglomerular baroreceptors in response to a reduction in perfusion pressure. Thus, persistent hyperreninemia, a high renovascular resistance, a computed reduction in ΔP , and a paucity of morphological evidence for tubular obstruction are all consistent with the presence of afferent vasoconstriction in the group 2 allografts of the present study. We propose that this alteration in segmental renovascular resistance could well be the proximate cause of posts ischemic filtration failure in the freshly transplanted kidney.

Appendix

A comparison was made between the simultaneous clearances of exogenous iothalamate and endogenous (true) creatinine in day 3 studies, during which the absence of interfering substances permitted iothalamate levels to be assayed. Linear regression analysis reveals the relationship between the two clearances to be strong, with a coefficient of correlation (R value) of 0.99 (Fig. 8). The method of Bland and Altman was used to evaluate the level of agreement between the two methods (47). The confidence interval of agreement was estimated by plotting the difference between simultaneous iothalamate and creatinine clearances as a function of the average of the two clearances. Among members of group 2 with hypofiltration, there was no bias between the methods. The mean value of iothalamate minus creatinine clearance was 0. The confidence interval of agreement (± 2 SD) was -3 to $+3$ ml/min. Surprisingly, among members of group 1 with normal GFR, a bias in favor of iothalamate was observed. The mean value for iothalamate minus creatinine clearance was $+6$ ml/min. This trend for iothalamate clearance to exceed creatinine clearance in group 1 is clearly evident by inspection of Fig. 8. The confidence interval of agreement between the two methods in group 1 subjects (± 2 SD) was -6 to $+18$ ml/min. Given the large average difference in GFR of 53 ml/min between groups 1 and 2 on

postoperative day 3 (Table VI), we submit that the level of agreement between iothalamate and creatinine clearance is sufficiently good to allow the latter to be used as a measure of GFR during the early evaluation of GFR on the operation day. We speculate that the tubular creatinine transporter could have been saturated at the high levels of serum creatinine that prevailed at the time of the day 3 study (5 ± 1 mg/dl). This would explain the apparent absence of a measurable tubular secretory component to the creatinine clearance under the conditions of our study.

Acknowledgments

This study was supported by grants DK 29985 and DK 20368 from the National Institutes of Health. Dr. Veludina Alejandro is the recipient of a fellowship from the Northern California Chapter of the National Kidney Foundation.

References

1. Hefty, T., S. Fraser, K. Nelson, W. Bennett, and J. Barry. 1992. Comparison of UW and Euro-Collins solutions in paired cadaveric kidneys. *Transplantation (Baltimore)*. 53:491-492.
2. Arendhorst, W. J., W. F. Finn, and C. W. Gottschalk. 1976. Micropuncture study of acute renal failure following temporary renal ischemia in the rat. *Kidney Int.* 10:S6:S100-S105.
3. Tanner, G. A., and S. Sophasan. 1976. Kidney pressures after temporary renal artery occlusion in the rat. *Am. J. Physiol.* 230:1173-1181.
4. Donohoe, J. F., M. A. Venkatasalam, D. B. Bernard, and N. G. Levinsky. 1978. Tubular leakage and obstruction after renal ischemia: structural-functional correlations. *Kidney Int.* 13:208-222.
5. Burke, T. J., R. E. Cronin, K. L. Duchin, L. N. Peterson, and R. W. Schrier. 1980. Ischemia and tubule obstruction during acute renal failure in dogs: mannitol in protection. *Am. J. Physiol.* 238:F305-F314.
6. Finn, W. F., and R. L. Chevalier. 1979. Recovery from posts ischemic acute renal failure in the rat. *Kidney Int.* 16:113-123.
7. Williams, R. H., C. E. Thomas, L. G. Navar, and A. P. Evan. 1981. Hemodynamic and single nephron function during the maintenance phase of ischemic acute renal failure in the dog. *Kidney Int.* 19:503-515.
8. Robinette, J. B., and J. D. Conger. 1990. Angiotensin and thromboxane in the enhanced renal adrenergic nerve sensitivity of acute renal failure. *J. Clin. Invest.* 86:1532-1539.
9. Myers, B. D., L. Newton, C. Boshkos, J. A. Macoviak, W. H. Frist, G. C. Derby, M. G. Perlroth, and R. K. Sibley. 1988. Chronic injury of human renal microvessels with "low dose" cyclosporine therapy. *Transplantation (Baltimore)*. 46:694-703.
10. Perico, N., P. Ruggenti, F. Gasparini, L. Mosconi, A. Benigni, C. Amuchastegui, F. Gasparini, and G. Remuzzi. 1992. Daily renal hypofusion induced by cyclosporine in patients with renal transplantation. *Transplantation (Baltimore)*. 54:56-62.
11. Myers, B. D., R. B. Nelson, W. G. Williams, P. H. Bennett, A. S. Hardy, R. L. Berg, N. Loon, W. C. Knowler, and W. E. Mitch. 1991. Glomerular function in Pima Indians with non-insulin-dependent diabetes mellitus of recent onset. *J. Clin. Invest.* 88:524-530.
12. Miller, T. R., R. J. Anderson, S. L. Linas, W. L. Henrich, A. S. Berns, P. A. Gabow, and R. W. Schrier. 1978. Urinary diagnostic indices in acute renal failure: a prospective study. *Ann. Intern. Med.* 89:47-50.
13. Myers, B. D., and S. M. Moran. 1986. Hemodynamically mediated acute renal failure. *N. Engl. J. Med.* 314:97-105.
14. Moran, S. M., and B. C. Myers. 1985. Course of acute renal failure studied by a model of creatinine kinetics. *Kidney Int.* 27:928-937.
15. Chagnac, A., B. A. Kiberd, M. C. Fariñas, S. Strober, R. K. Sibley, R. Hoppe, and B. D. Myers. 1989. Outcome of the acute glomerular injury in proliferative lupus nephritis. *J. Clin. Invest.* 84:922-930.
16. Guasch, A., M. Suranyi, L. Newton, B. M. Hall, and B. D. Myers. 1992. Extent and course of glomerular injury in human membranous glomerulopathy. *Am. J. Physiol.* 263 (*Renal Fluid Electrolyte Physiol.* 32):F1034-F1043.
17. Weibel, E. 1979. *Stereological Methods. Vol. 1. Practical Methods for Biological Morphometry.* Academic Press Ltd., London.
18. Drummond, M. C., B. Kristal, B. D. Myers, and W. M. Deen. 1994. Structural basis for reduced glomerular filtration capacity in nephrotic humans. *J. Clin. Invest.* 94:1187-1195.
19. Jensen, E. B., H. J. G. Gundersen, and R. Osterby. 1979. Determination of membrane thickness distribution from orthogonal intercepts. *J. Microsc. (Oxf.)*. 115:19-33.
20. Canaan-Kuhl, S., E. S. Venkatraman, S. I. B. Ernst, R. A. Olshen, and B. D. Myers. 1993. Relationships among protein and albumin concentrations and

oncotic pressure in nephrotic plasma. *Am. J. Physiol.* 264 (Renal, Fluid and Electrolyte Physiology 33):F1052–1059.

21. Dunnill, M. S., and W. Halley. 1973. Some observations on the quantitative anatomy of the kidney. *J. Pathol.* 110:113–121.

22. Drumond, M. C., and W. M. Deen. 1994. Structural determinants of glomerular hydraulic permeability. *Am. J. Physiol.* 266:F1–F12.

23. Drumond, M. D., and W. M. Deen. 1994. Stokes flow through a row of cylinders between parallel walls: model for the glomerular slit diaphragm. *J. Biomech. Eng.* 116:184–189.

24. Deen, W. M., C. R. Robertson, and B. M. Brenner. 1972. A model of glomerular ultrafiltration in the rat. *Am. J. Physiol.* 223:1178–1183.

25. Battilana, C., H. Zhang, R. Olshen, L. Wexler, and B. D. Myers. 1991. PAH extraction and the estimation of plasma flow in the diseased human kidney. *Am. J. Physiol.* 30:F726–F733.

26. Bull, G. M., A. M. Joekes, and K. G. Lowe. 1950. Renal function studies in acute tubular necrosis. *Clin. Sci. (Lond.)* 9:379–404.

27. Myers, B. D., C. Miller, J. Mehigan, C. Olcott, H. Golbetz, C. R. Robertson, G. Derby, R. Spencer, and S. Friedman. 1984. Nature of the renal injury following total renal ischemia in man. *J. Clin. Invest.* 73:329–341.

28. Solez, K., L. Morel-Maroger, and J. D. Sraer. 1979. The morphology of “acute tubular necrosis” in man: analysis of 57 renal biopsies and a comparison with glycerol model. *Medicine (Baltimore)*. 58:362–376.

29. Jones, D. B. 1982. Ultrastructure of human acute renal failure. *Lab. Invest.* 46:254–264.

30. Stein, J. H. 1977. The glomerulus in acute renal failure. *J. Lab. Clin. Med.* 90:227–230.

31. Nyengaard, J. R., and T. F. Bendtsen. 1992. Glomerular number and size in relation to age, kidney weight, and body surface in normal man. *Anat. Rec.* 232:194–201.

32. Eisenbach, G. M., and M. Steinhausen. 1973. Micropuncture studies after temporary ischemia of rat kidneys. *Pflug. Arch. Eur. J. Physiol.* 343:11–25.

33. Yagil, Y., B. D. Myers, and R. L. Jamison. 1988. Course and pathogenesis of post-ischemic acute renal failure in the rat. *Am. J. Physiol.* 24:F257–F264.

34. Meyer, T. W., and H. Rennke. 1988. Progressive glomerular injury after limited renal infarction in the rat. *Am. J. Physiol.* 254(Renal Fluid Electrolyte Physiol. 23):F856–F862.

35. Solez, K., L. C. Racusen, N. Marcussen, I. Slatnik, P. Keown, J-F. Burdick, and S. Olsen. 1993. Morphology of ischemic acute renal failure, normal function, and cyclosporine toxicity in cyclosporine-treated renal allograft recipients. *Kidney Int.* 43:1058–1067.

36. Oliver, J., M. MacDowell, and A. Tracy. 1951. Pathogenesis of acute renal failure associated with traumatic and toxic injury: renal ischemia, nephrotoxic damage and the ischemic episode. *J. Clin. Invest.* 30:1305–1351.

37. Olsen, S., J. F. Burdick, P. A. Keown, A. C. Wallace, L. C. Racusen, and K. Solez. 1989. Primary acute renal failure (“acute tubular necrosis”) in the transplanted kidney: morphology and pathogenesis. *Medicine (Baltimore)*. 68:173.

38. Schnermann, J. 1975. Regulation of single nephron filtration rate by feedback: facts and theories. *Clin. Nephrol.* 3:75–81.

39. Alejandro, D., J. Nelson, R. Sibley, D. Dafoe, E. Alfrey, J. Scandling, and B. Myers. 1993. Regulation of Na⁺ transport by the post ischemic human kidney. *J. Am. Soc. Nephrol.* 4:311.

40. Brown, J. J., R. L. Gleadle, D. H. Lawson, A. F. Lever, A. L. Linton, R. F. Macadam, E. Prentice, M. Tree, and J. J. Robertson. 1970. Renin and acute renal failure: studies in man. *Br. Med. J.* 1:253–258.

41. Tu, W. H. 1965. Plasma renin activity in acute tubular necrosis and other renal diseases associated with hypertension. *Circulation.* 31:686–695.

42. Myers, B. D. 1986. Nature of postischemic renal injury following aortic or cardiac surgery. In *Acute Renal Failure in the Intensive Therapy Unit, Acute Renal Failure Workshop*. Springer-Verlag, Avignon, France. pp. 167–180.

43. Kon, V., T. Yoshioka, A. Fogo, and I. Ischikawa. 1989. Glomerular actions of endothelin in vivo. *J. Clin. Invest.* 83:1762–1767.

44. Moore, K., J. Wendon, M. Frazer, J. Karani, R. Williams, and K. Badr. 1992. Plasma endothelin immunoreactivity in liver disease and the hepatorenal syndrome. *N. Engl. J. Med.* 327:1774–1778.

45. Dibona, G. 1987. Renal innervation and denervation: lessons from renal transplantation reconsidered. *Artif. Organs.* 11:457–462.

46. Holmer, S., B. Rinne, K. Eckardt, M. Le Hir, K. Schrickler, B. Kaissling, G. Riegger, and A. Kurtz. 1994. Role of renal nerves for the expression of renin in adult rat kidney. *Am. J. Physiol.* 266 (Renal Fluid Electrolyte Physiol. 35):F738–F745.

47. Bland, J. M., and D. G. Altman. 1986. Statistical methods for assessing agreement between two methods of clinical measurement. *Lancet.* i:307–310.